

## Application of Multidimensional Magnetic Sensors —Position and Movement Detection—

Kazusuke Maenaka, Yuichiro Shimizu, Makoto Baba and Muneo Maeda

Department of Electronics,  
Himeji Institute of Technology,  
Shosha 2167, Himeji, Hyogo 671-22, Japan

(Received May 10, 1995; accepted August 16, 1995)

**Key words:** magnetic field sensor, multidimensional sensing, neural processing, position sensing, movement detection

This paper deals with one of the applications of multidimensional magnetic sensors. Since the magnetic field is a vector quantity and a function of the relative position of the magnetic source, the position and/or movement of an object around the magnetic source can be detected by measurement of the field vector at the object. In this paper, a two-dimensional magnetic sensor with neural signal processing is used for this detection. Two examples of actual position and movement detection are described: one is parallel movement in a plane and the other is finger movement. Both these cases were realized in real time, with error of less than 4–5 percent.

### 1. Introduction

Conventional magnetic sensors in general detect one component of a magnetic field. However, there are many applications where the simultaneous detection of more than one component of the magnetic field vector is required. Examples include angle detectors, omnidirectional magnetic measurements, and nondestructive inspections based on field leakage. For such applications, many types of novel multidimensional magnetic sensors have been reported. These sensors were usually fabricated with integrated circuit technology because of spatial resolution, assembling accuracy, mass reproducibility and possibility of future development of intelligent sensors. The literature on silicon magnetic sensors including reviews is listed in refs. 1 to 8. Applications of multidimensional magnetic sensors have also been reported, i.e., the angle sensor<sup>(9)</sup> and the omnidirectional sensor.<sup>(10)</sup>

In this paper, we will introduce one more application, a position and movement detection system, which utilizes a multidimensional magnetic sensor.

A position and movement detection system using magnetic field as an intermediate carrier has already been established by McDonnell-Douglas,<sup>(1)</sup> where a set of three-dimensional coils is used as the magnetic source and detector. This system is rather complex, and has a large magnetic source and detector size (about 10,000 mm<sup>3</sup>) because of the three-dimensional coils, resulting in inappropriateness for the detection of small moving objects or nonrestrictive measurements. Moreover, since the magnetic source and detector must be regarded as points because of the mathematical conversion from the magnetic field into position, the shape of the magnetic source and detector must be fixed.

This paper deals with a position and movement detection system using a permanent magnet and a solid-state magnetic sensor as the magnetic source and the detector, respectively. The conversion from magnetic field to position is performed by neural signal processing. This enables the nonrestrictive measurement of the movement because the magnet requires no wiring. Moreover, irregularly shaped magnetic sources and detectors can be used because of the universality of neural signal processing. In this paper, the concept of our system and examples of position and movement detection will be discussed.

## 2. Concept of Position Sensing

The magnetic field vector around a magnetic source is a function of the relative position of the magnetic source. If the one-to-one correspondence between an arbitrary position and the magnetic field at that point is assumed, the position can be inversely calculated by the measured magnetic field at that position. Figure 1 shows a position detection system based on the above concept. The permanent magnet as the magnetic source is fixed at the origin and the multidimensional magnetic sensor is attached to an object, the position of which will be determined. This setting is, of course, interchangeable, i.e., the magnetic sensor is fixed at the origin and the magnet is attached to the object. This interchangeability enables the object to be free from restriction of the electrical leads from the magnetic sensor, and a small, lightweight or thin magnet film can be used for a small object moving in a small area. For simplicity, we will assume in this paper that the magnetic source is fixed at the origin.

Assuming a magnetic microdipole as the magnetic source, the magnetic field distribution around the magnetic source is described as

$$B_x = \frac{M}{4\pi} \frac{3xy}{(x^2 + y^2 + z^2)^{5/2}} \quad (1a)$$

$$B_y = \frac{M}{4\pi} \frac{(2y^2 - x^2 - z^2)}{(x^2 + y^2 + z^2)^{5/2}} \quad (1b)$$

$$B_z = \frac{M}{4\pi} \frac{3yz}{(x^2 + y^2 + z^2)^{5/2}} \quad (1c)$$

where  $M$  is the magnetic dipole moment. The magnetic flux density reduces as  $(1/\text{distance})^{3-4}$  from the magnetic source. This implies that this method of position sensing is suitable for small areas, within  $100 \text{ mm}^3$  by using a conventional magnet and solid-state magnetic sensor, since the magnetic field rapidly decreases with increasing distance.

Essentially, the inverse functions of eq. (1),  $x = f(B_x, B_y, B_z)$ , provide the position of an object from the measured magnetic field at the object. Actually, the system reported in ref. 11 uses these mathematical relations.

Equation (1) is valid only when the magnetic source and detector are regarded as points. For convenience of system design, the shape of the magnetic source and detector should be varied for the application in question, i.e., when the magnet is used as the magnetic source, a large and strong magnet is preferable for wide-range measurements and a small, light or thin magnet is desirable for nonrestrictive measurements. In these cases, the magnetic source cannot be regarded as a point and eq. (1) and its inverse function are no longer valid. Although the numerical relationship between the position and magnetic field can be resolved by FEM for any shape of the magnetic source, it is troublesome and ineffective. We use neural signal processing for this inverse operation which converts the magnetic field into the position.

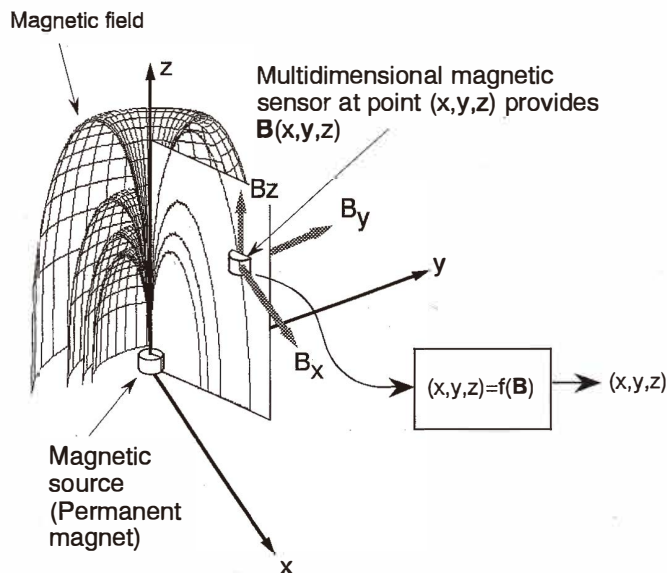


Fig. 1. Schematic diagram of novel position/movement detection system.

### 3. Neural Signal Processing (NSP)

Recently, neural signal processing (NSP)<sup>(12)</sup> has been widely used for realizing various functions which are adaptively built up by repeatedly applying teaching data, in particular, digital functions such as character recognition. The universality of NSP is suitable for our purpose. Once a set of predetermined relationships between the position and the magnetic field at that position is input to NSP as teaching data, NSP provides position data from the measured magnetic field even if the measured data are not included in the teaching data. The merits of this method are that: (i) any shape of magnetic source may be used, (ii) any type of detector can be employed, which means that spatial resolution and cross-sensitivity of the magnetic sensor are not important terms, and (iii) any movement, such as the movement of an arm with joint, can be detected (with a few limitations, as described in Section 5).

NSP includes several layers of neural elements, as shown in Fig. 2. An output of a neural element is connected to another element in the next layer with individual weights,  $w_{ji}$ . With the teaching data, the weights successively converge to a certain value so that NSP provides the required function. Although many types of NSP are suggested for improvement of learning efficiency and accuracy, a simple and fundamental NSP is used here.

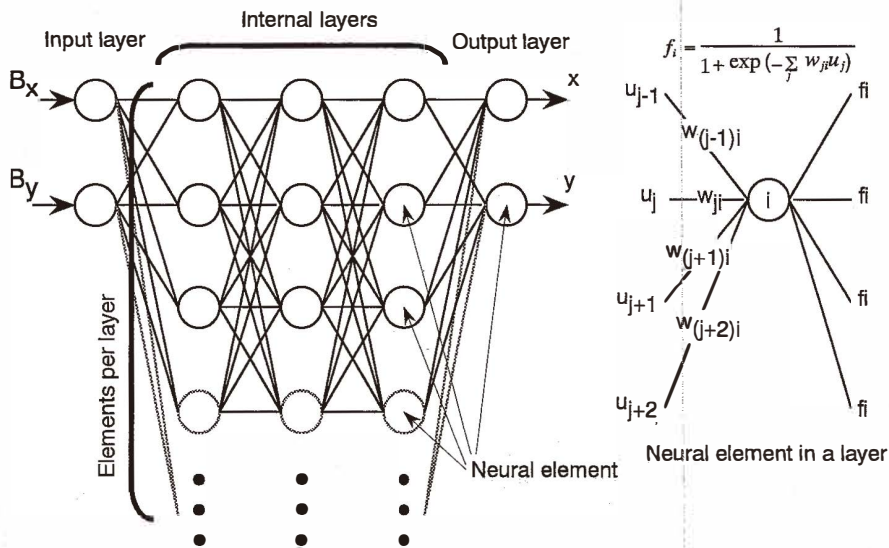


Fig. 2. Structure of neural network and neural element (neuron).

The NSP used here has two-inputs, two-outputs and three internal layers, with 5–10 elements per layer, and no-feedback connections. The transfer function of the neural elements is a common sigmoidal function,  $f_i(\mathbf{u}) = (1 + \exp(-\sum w_{ji} u_j))^{-1}$ . The input and output signals are analog signals, the ranges of which are normalized between 0.1 and 0.9, in order to reduce errors in the vicinity of 0 and 1 output of the neural elements. The internal configuration (number of layers and elements per layer) of the NSP must be optimized with respect to application by trial and error. The learning algorithm is a common back-propagation method with the acceleration and inertia terms.

As teaching data to NSP, the relationship between the position and the magnetic field at that position must be clarified by a preliminary measurement. Over a defined area of the movement, the components of the magnetic field vector,  $B_x$  and  $B_y$ , are measured for each position to be learned. The suitable number and selection of the teaching data depend on the required accuracy, nonlinearity, and allowed learning time (the learning time is long for a large number of teaching data). Thus the teaching data should be properly selected for high-quality calculation. At present, we use a simple set of teaching data, which are measured at evenly divided points (about 10 to 20 divisions) of a defined area of the movement.

#### 4. Examples of Sensing

When we use a two (three)-dimensional magnetic sensor for the magnetic detection, the calculated position becomes two (three)-dimensional. In other words, the number of degrees of freedom is limited by the dimensional detection ability of the magnetic sensor. In our examples, a two-dimensional magnetic sensor is used, and two degrees of freedom are allowed for movement. Various types of movement can be considered, such as parallel movement in a plane, movement of two arms with two joints in a plane, rotation along two axes at a fixed point, and movement along an arbitrary curve with rotation along an axis, as shown in Fig. 3.

As examples of our method, two types of movements, Figs. 3(a) and 3(b), were examined.

##### 4.1 *Parallel movement in a plane*

The detection of the parallel movement in a plane is examined. A permanent magnet is fixed at the origin and a two-dimensional magnetic sensor is attached on the object moving in parallel. For the two-dimensional magnetic detector, two Hall cells which are fixed at right angles to each other were used.

At first, the magnetic field components,  $B_x$  and  $B_y$ , as a function of position  $(x, y)$  were measured in order to acquire the teaching data. The magnet for the experiments has a diameter of 17 mm, thickness of 4 mm, and magnetic flux density of 0.22 T at the surface (SmCo magnet). The size of the two-dimensional magnetic sensor is about  $4 \times 4 \times 4 \text{ mm}^3$  including the package. The sensitivity of the magnetic detector is set to 0.1 V/T by adjusting the gain of the following DC amplifier. The r.m.s. noise level in the magnetic detectors corresponds to about  $10 \mu\text{T}$ .

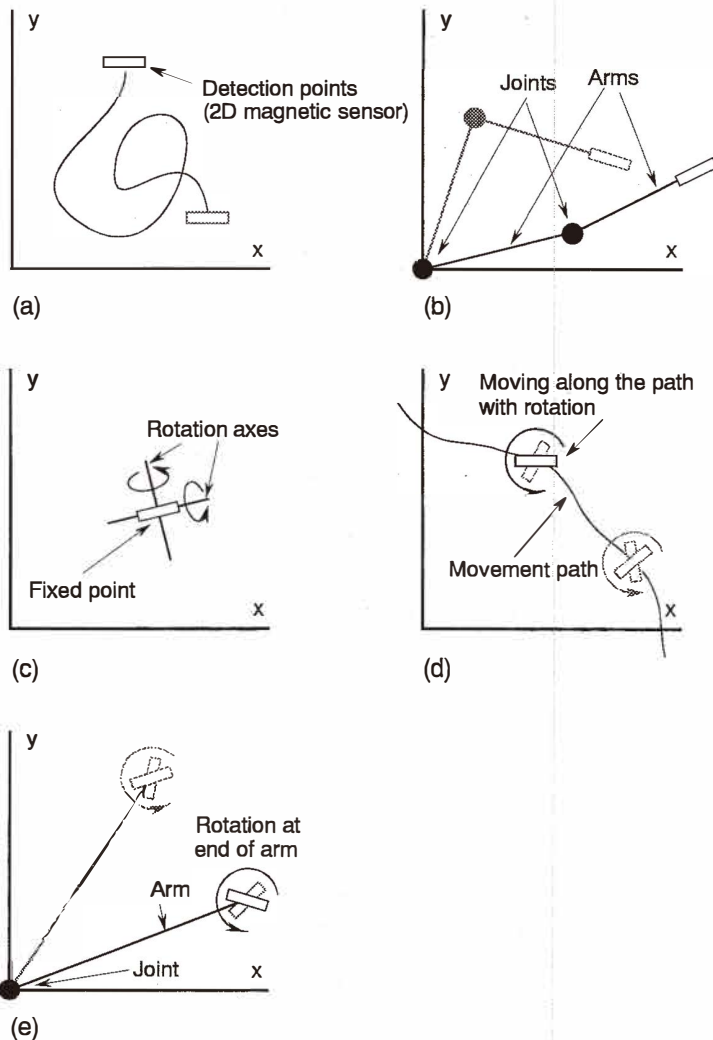


Fig. 3. Examples of moving object on a plane (two degrees of freedom): (a) parallel movement, (b) movement of two arms with joints, (c) rotation along two axes, (d) movement along arbitrary curve with rotation, and (e) rotation at end of arm with joint.

The measured ranges of  $x$  and  $y$  were 4 to 50 and 0 to 46 mm, respectively, where the measurement for  $y < 4$  mm was not carried out because of magnetic sensor size restrictions. The interval of the measurements in the  $x$  and  $y$  directions is 2 mm each (total number of teaching data is  $24 \times 24 = 576$ ). From the measured magnetic field components  $B_x(x,y)$  and  $B_y(x,y)$ , the points  $(x,y)$  are plotted in Fig. 4, where the intersecting points of the mesh

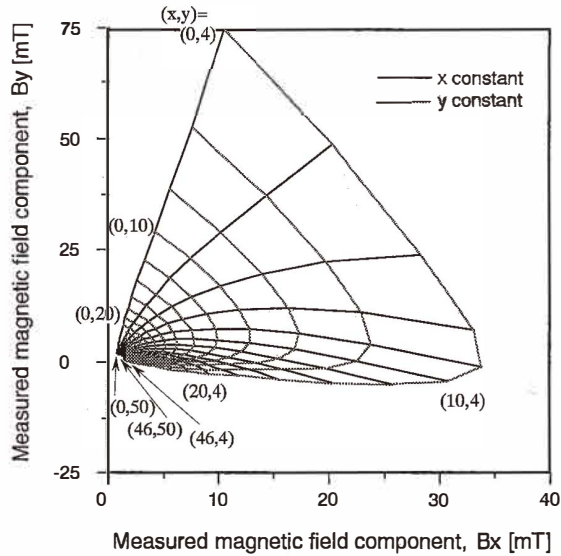


Fig. 4. Measured magnetic fields  $B_x$  and  $B_y$  vs. positions  $x$  and  $y$ .

indicate measured points or teaching points. This figure (conversion map) shows a sudden change of the magnetic field as the measured point changes. There is high nonlinearity between the magnetic field  $B(x,y)$ , and the point  $(x,y)$  and the size of mesh is too small for large values of  $x$  and  $y$ .

In order to reduce the nonlinearity for good learning, the data are compressed before inputting to the NSP. The compression can be done by the following pseudo-log operations,

$$B_x' = \text{sign}(B_x) \cdot \log(\text{abs}(B_x) \times \alpha_x + \beta_x) \quad (2a)$$

$$B_y' = \text{sign}(B_y) \cdot \log(\text{abs}(B_y) \times \alpha_y + \beta_y) \quad (2b)$$

where  $\text{sign}(B)$  and  $\text{abs}(B)$  indicate the sign and absolute operations, respectively, and  $\alpha$  and  $\beta$  are constants.  $\alpha$  and  $\beta$  were chosen to generate an appropriate data set. Values of the constants are  $\alpha_x = 25$ ,  $\beta_x = 0$ ,  $\alpha_y = 1000$ , and  $\beta_y = 1$ , which were chosen by trial and error. After the compression, the conversion map approaches a uniform mesh as shown in Fig. 5.

The measured data ( $x$  and  $y$  versus  $B_x'$  and  $B_y'$ ; 576 data set) are input to the NSP with 3 middle layers and 5 elements per layer as the teaching data. The teaching algorithm is a common back-propagation algorithm with acceleration and inertia coefficients of 0.5. After 100,000 iterations, the relative r.m.s. error was reduced to 4.6% as shown in Fig. 6. The conversion map of NSP, which has a similar form as Fig. 5, is shown in Fig. 7, where

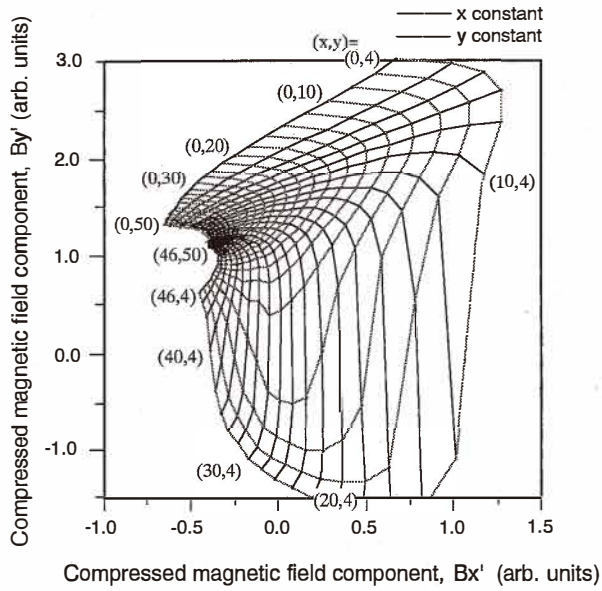


Fig. 5. Magnetic fields  $B_x'$  and  $B_y'$  vs. positions  $x$  and  $y$  after compression.

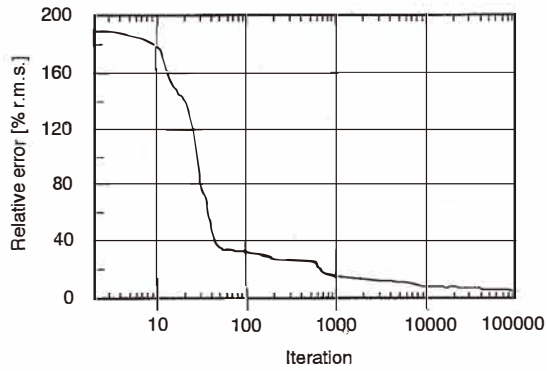


Fig. 6. Learning curve of NSP.



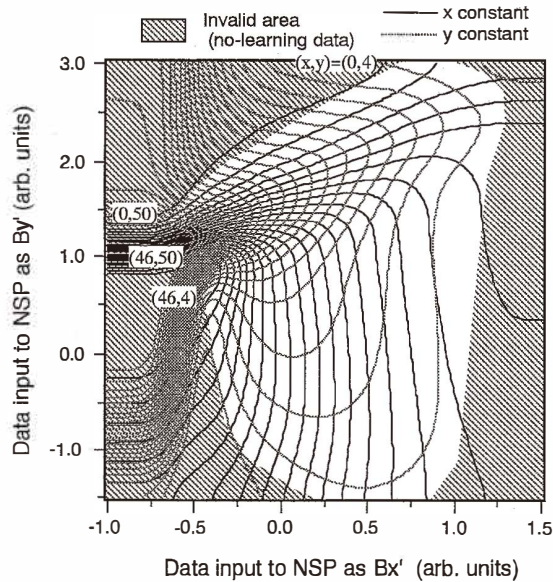


Fig. 7. Conversion map of NSP.

the hatched area is invalid because of the absence of teaching data. From a comparison with Fig. 5, it was found that NSP simulates well the relation between the magnetic field and position. The error map for the defined area is shown in Fig. 8. The error increases at the two regions of small  $y$  and small  $x$ . The reason for the increase at the region of small  $y$  is that the magnetic component for the  $x$  direction,  $B_x$ , is too small around  $y = 0$ , resulting in less information for NSP learning. As for the increase at the region of small  $x$ , the change of  $B_x$  with respect to the change of  $x$  position is small because the magnetic source has a relatively large surface in the  $x$  direction.

In conclusion, our system is applicable to position detection in which an error of several percent is allowable and the detected area is less than  $50 \text{ mm}^2$ . As for the learning error, further experiments implied that the r.m.s. error can be reduced even more by optimizing the design of the NSP structure and the learning algorithm. Work on these is in progress.

#### 4.2 Bending angle detection

A virtual reality system needs to detect the movement or bending angle of fingers in real time. Our system meets this requirement.

Figure 9 shows the joints of a human hand. The thumb has an interphalangeal joint (IP joint) and a metacarpophalangeal joint (MP joint). The other four fingers have a distal interphalangeal joint (DIP joint), a proximal interphalangeal joint (PIP joint) and a MP joint. Each DIP joint, PIP joint and IP joint has one degree of freedom while the MP joint

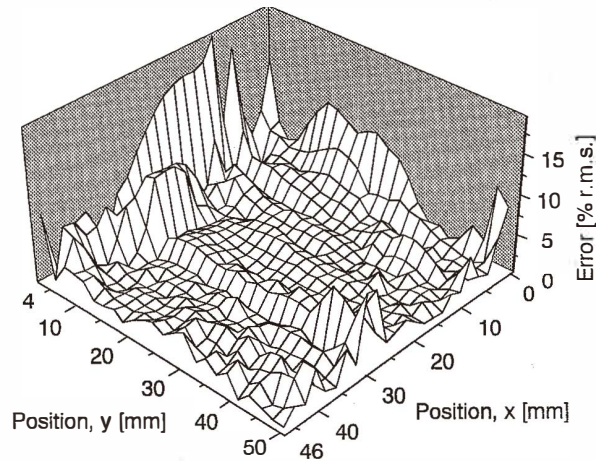


Fig. 8. Error map of NSP for defined area.

has two degrees of freedom. Four degrees of freedom are required to completely describe the movement of each finger. In our experiments, however, the measurement of the movement is limited to two degrees of freedom for each finger. Since the DIP joint has no muscle and it cannot move by itself<sup>(13)</sup> (the movement of the DIP joint depends on that of the PIP joint), the detection of two degrees of freedom is suitable for the free movement of fingers in a plane.

In the system, a cylindrical magnet is attached to the palm or back of the hand, and a two-dimensional magnetic sensor is attached onto the DIP joint as shown in Fig. 10. When the PIP and MP joints of the finger are bent at angles of  $\theta_1$  and  $\theta_2$ , respectively, the two-dimensional magnetic sensor detects magnetic components  $B_V$  and  $B_H$  at the DIP joint. The detected magnetic components are directly (without compression) applied to NSP. The NSP in this system has 2-inputs and 2-outputs, 3 middle layers and 10 elements per layer. The teaching data are obtained by measuring the magnetic field components at 15 deg. intervals for each of the two bending angles,  $\theta_1$  and  $\theta_2$ . Learning of the neural network was done 100,000 times with an acceleration coefficient of 0.7 and an inertia coefficient of 0.9.

The conversion map and error map of NSP are shown in Figs. 11 and 12, respectively. The final average error is 0.17 degrees. The response time of this system, which is the time of the forward propagation of the NSP, is satisfied with real-time processing. The operations for the conversion from the sensor outputs ( $B_V, B_H$ ) into the bending angles ( $\theta_1, \theta_2$ ) include 424 floating point multiplications, 424 floating point additions and 42 exponential calculations. This conversion takes 1/50 s on a Macintosh PowerBook 180c, laptop computer, meaning that real-time measurement can be achieved.

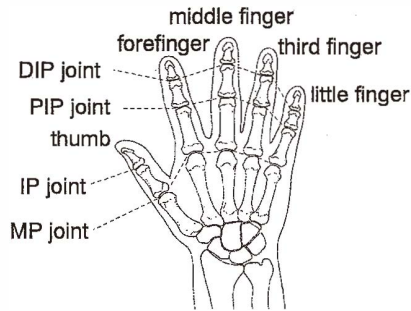


Fig. 9. Human hand.

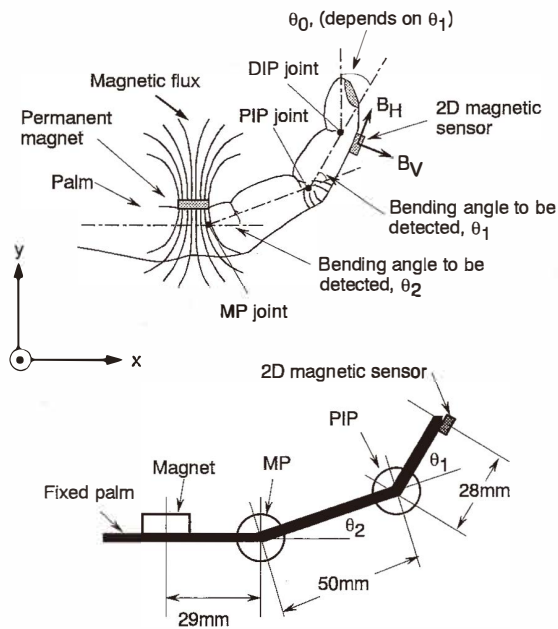


Fig. 10. Detection of bending angle for finger.

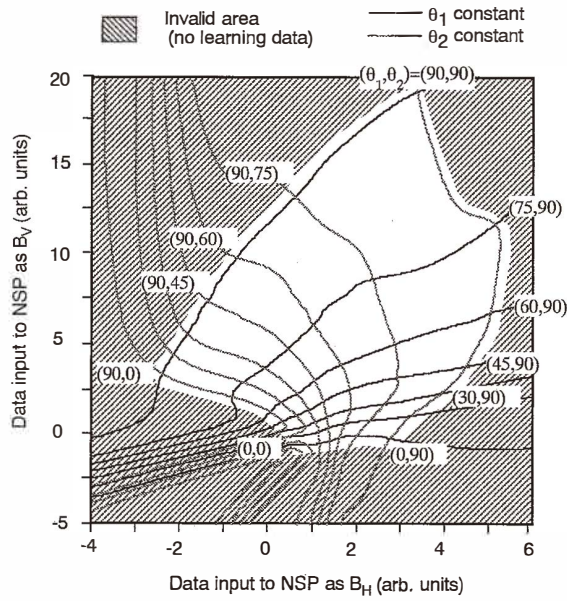


Fig. 11. Conversion map of NSP.

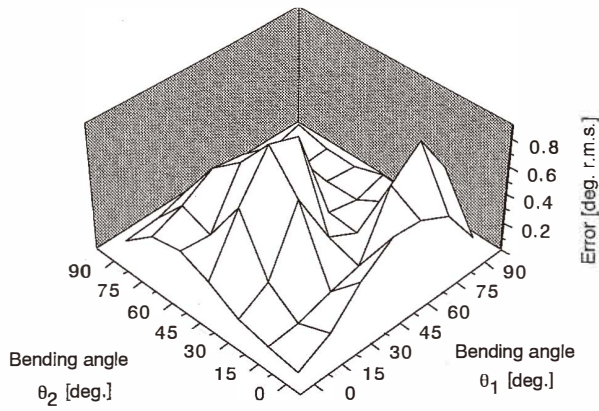


Fig. 12. Error map of NSP.

## 5. Possibilities and Limitations of the System

Two examples were shown above. The combination of the multidimensional magnetic sensor and neural signal processing has many possibilities for application to position and movement detection. In this section, we discuss the possibilities and limitations of the system.

As described in section 4, the highly nonlinear function can be simulated by practical neural networks. This is valid even if the shapes of the magnetic source and magnetic detector are irregular. This implies that an arbitrary shape of the magnet which fits the shape of the moving object can be used. Moreover, the spatial resolution, individuality or orthogonality of the sensing axis, and sensitivity difference for each axis of the multidimensional magnetic sensor is not important. This is a merit for using multidimensional magnetic sensors which have poor orthogonality and spatial resolution.

Although our examples show only the detection of movement for one object, the detection of movement of many objects around the magnetic source can be achieved by installing a magnetic detector on each object. In this case, the movement of the object is limited by the cables from the magnetic sensor, although flexible cables are now available and can be used for some applications.

In this paper, an NSP with two inputs and two outputs was used. However, an NSP with three inputs and three outputs can also be used. This allows direct expansion of the degrees of freedom for detection without any essential difficulty except for the increase of preliminary measurement points or number of teaching data.

Our method has two limitations. First, the S/N ratio of the magnetic sensor restricts the size of the detection area. The magnetic flux density is less than 0.1 mT at a point 50 mm from the magnet with surface magnetic flux density of 0.2 T. This is close to the detection limit of solid-state magnetic sensors. Next is the theoretical limitation of the detection of motion. The former is resolved by developing novel device structures and operation principles, such as a coil-based magnetic sensor.<sup>(14)</sup> The latter is essentially unavoidable, and the details are described as follows.

Our method assumes the existence of a one-to-one correspondence between a point and the magnetic field at that point. This assumption is valid for many cases such as parallel movement and movement of two arms and joints similar to finger movements. However, this assumption is invalid in the case of movement along a curve with free rotation (see Fig. 3(d)), for example. If free rotation, 0 to 360 deg. rotation, is allowed, there is a possibility that the one-to-one correspondence becomes invalid. That is, if there are more than two positions for which the absolute value of the magnetic flux density is equal, the calculated point from the magnetic field components is no longer unique. This may be solved by using a magnetic detector which has poor spatial resolution, because the rotation of the detector affects the absolute value of the magnetic field. Unfortunately, we cannot find a general solution for movement with one-to-one correspondence. However, one-to-one correspondence can be checked by examining whether the mesh of the conversion map, such as that in Fig. 4, is twisted or not in the defined area.

## 6. Conclusions

The position and movement detection method using a multidimensional magnetic sensor was discussed. The conversion from magnetic field to position is performed by neural signal processing. The neural signal processor simulates well the conversion function although the function is highly nonlinear. This method is suitable for the detection of position and movement in small areas with no constraints, such as monitoring of the movement of micromachines, or clinical examination of movement of tongue and eyeball.

## Acknowledgments

The authors wish to thank the late Professor T. Nakamura who opened new vistas of multidimensional and integrated magnetic sensors, and his colleagues at Toyohashi University of Technology who collaborated with us. Finally, we pray for the repose of Professor Nakamura's soul.

This work was supported in part by a Grant-in-Aid (No. 06452232) from the Ministry of Education, Science and Culture of Japan.

## References

- 1 Lj. Ristic and M. Paranjape: *Sensors and Materials* **5** (1994) 301.
- 2 V. Zieren and S. Middelhoek: *Sensors and Actuators* **2** (1982) 251.
- 3 S. Kordic and P. J. A. Munter: *IEEE Transactions on Electron Devices* **ED-35** (1988) 771.
- 4 M. Paranjape, I. Filanovsky and Lj. Ristic: *Sensors and Actuators* **A34** (1992) 9.
- 5 K. Maenaka, T. Ohgusu, M. Ishida and T. Nakamura: *Trans. IEE of Japan* **109-C** (1989) 483 (in Japanese).
- 6 Ch. S. Roumenin: *Sensors and Actuators* **A24** (1990) 83.
- 7 H. P. Baltes and R. S. Popovic: *Proc. IEEE* **74** (1986) 1107.
- 8 S. Kordic: *Sensors and Actuators* **10** (1986) 347.
- 9 K. Maenaka, M. Tsukahara and T. Nakamura: *Sensors and Actuators* **A21-A23** (1990) 747.
- 10 K. Maenaka, T. Ohgusu and T. Nakamura: *IEICE Trans.* **J74-C-II** (1991) 325 (in Japanese).
- 11 Trade name "3 SPACE," McDonnell-Douglas: U. S. Patent 3 868 565
- 12 D. E. Rumelhart and J. L. McClelland: *Parallel Distributed Processing* (Vol. I MIT Press, Cambridge, 1986).
- 13 R. Tubiana, J. M. Thomine and E. Mackin: *Examination of the Hand & Upper Limb* (Saunders Co., Philadelphia, 1984).
- 14 S. Kawahito, Y. Sasaki, M. Ishida and T. Nakamura: *Sensors and Materials* **5** (1994) 241.